Substrate quality drives fungal necromass decay and decomposer community structure under contrasting vegetation types

Authors: Katilyn V. Beidler[1*], Richard P. Phillips[1], Erin Andrews[2,3], François Maillard[2], Ryan M. Mushinski[1,4] and Peter G. Kennedy[2]

1. Department of Biology, Indiana University Bloomington, IN 47405
2. Department of Plant and Microbial Biology University of Minnesota St. Paul, MN 55108
3. Department of Ecology & Evolutionary Biology, University of Tennessee Knoxville, 37996
4. School of Public & Environmental Affairs, Indiana University Bloomington, IN 47405

Corresponding author: Katilyn V. Beidler , Email: kbeidler@indiana.edu,
Phone: (812) 856-1563, Address: Jordan Hall, 1001 East Third Street, Room JH234,
Bloomington IN 47405, USA

Abstract

1. Fungal mycelium is increasingly recognized as a central component of soil biogeochemical cycling, yet our current understanding of the ecological controls on fungal necromass decomposition is limited to single sites and vegetation types.

2. By deploying common fungal necromass substrates in a temperate oak savannah and hardwood forest in the midwestern USA, we assessed the generality of the rate at which high- and low-quality fungal necromass decomposes; further, we investigated how the decomposer 'necrobiome' varies both across and within sites under vegetation types dominated by either arbuscular (AM) or ectomycorrhizal (EM) plants.

3. The effects of necromass quality on decay rate were robust to site and vegetation type differences, with high-quality fungal necromass decomposing, on average, 2.5 times faster during the initial stages of decay. Across vegetation types, bacterial and fungal communities present on decaying necromass differed from bulk soil microbial communities and were influenced by necromass quality. Moulds, yeasts and copiotrophic bacteria consistently dominated the necrobiome of high-quality fungal substrates.

4. Synthesis: We show that regardless of differences in decay environments, high-quality fungal substrates decompose faster and support different types of decomposer microorganisms when compared with low-quality fungal tissues. These findings help to refine our theoretical understanding of the dominant factors affecting fast cycling

components of soil organic matter (SOM) and the microbial communities associated with rapid decay.

Keywords: fungal hyphae, fungal mycelium, mycorrhizal type, oak savannah, temperate forest, necrobiome, melanin

Introduction

The amount of carbon (C) stored in soils is dependent upon the balance between soil organic matter (SOM) inputs and their subsequent rates of decomposition and C loss (Chapin *et al.*, 2011). While plant-derived inputs and losses have received decades of study (Berg & McClaughtery, 2014), there is growing evidence that fungal mycelium is also a major determinant of soil C stocks (Godbold *et al.*, 2006; Ekblad *et al.*, 2013; Clemmensen *et al.*, 2013; Zhang *et al.*, 2019). Conservative estimates of fungal mycelial biomass range from 20-250 g m^{-2}, with turnover times ranging from 9-48 days (Godbold *et al.*, 2006; Allen & Kitajima, 2014; Soudzilovskaia *et al.*, 2015). Moreover, once fungal biomass dies (i.e. becomes necromass), its decays rapidly (decay rate: 6.76 to 15.6 yr^{-1}; Zhang, Hui, Luo, & Zhou 2008; Brabcová, Štursová, & Baldrian 2018) and is rapidly assimilated into living microbial biomass (Drigo, Anderson, Kannangara, Cairney, & Johnson 2012; Miltner, Bombach, Schmidt-Brücken, & Kästner 2012; Lopez-Mondejar *et al.*, 2018). The high nutrient content of fungal necromass compared to other organic matter (OM) inputs also makes it an important resource for a variety of decomposers (Finlay & Clemmensen, 2016; Brabcová *et al.*, 2018). Recent studies indicate that the presence of fungal necromass significantly increases microbial enzyme activity (Zeglin & Myrold, 2013; Brabcová, Nováková, Davidová, & Baldrian 2016) and is responsible for up to 80% of nitrogen (N) cycling associated with the decomposition of belowground OM inputs (Zhang *et al.*, 2019).

Given the importance of soil fungi to C and nutrient cycling, there is a pressing need to understand the factors that control the fate of fungal necromass across diverse environments (Fernandez, Langley, Chapman, McCormack, & Koide 2016; Baskaran et al., 2017; Smith & Wan, 2019; Zhang *et al.*, 2019). Current knowledge of the controls on decomposition are largely derived from

assessments of plant litter decay, which identify the following interrelated factors: (1) climate; (2) biochemical traits (which typically indicate resource quality for decomposers); (3) soil properties (e.g. moisture, pH, and nutrient availability); and (4) decomposer community composition (Tenney & Waksman, 1926; Prescott, 2010; Berg & McClaugherty, 2014). Although there are no studies comparing fungal necromass decomposition along climatic gradients, fungal necromass has been shown to decompose faster when exposed to experimentally elevated temperatures (Fernandez *et al*., 2019), suggesting altered climatic conditions can influence the decomposition dynamics of this OM pool. At local scales, biochemical traits have been shown to be important predictors of fungal necromass decay and correspond with metrics of plant litter quality (Hurst & Wagner, 1969; Ekblad *et al.,* 1998; Cleveland *et al.,* 2014; Fernandez *et al.,* 2016). Specifically, both N and cell wall melanin content have been identified as key biochemical traits driving rates of fungal necromass decomposition (Koide & Malcom, 2009; Fernandez & Koide, 2012, 2014; Brabcová *et al.,* 2018; Lenaers *et al.,* 2018). Fungal tissues with a high melanin and low N content (*i.e*., low-quality substrates) tends to decay more slowly, when compared with fungal tissues with low melanin and high N content (high-quality substrates). In this way, melanin:N ratios in fungal necromass parallel lignin:N ratios in plant litter, which can be broadly predictive of decay rate (Melillo, Aber, & Muratore, 1982; Strickland Osburn, Lauber, Fierer, & Bradford 2009; Fernandez *et al.,* 2016). Unlike plant litter decay, however, it is not yet understood how site environmental conditions interact with initial substrate quality to control the rate at which fungal necromass decomposes.

In addition to climate and substrate quality, it's well-established that litter decay is also influenced by the biotic and abiotic properties of the soil, which are controlled in large part, by the dominant

vegetation (Hooper & Vitousek, 1997; Eviner & Chapin 2003, McLaren & Turkington 2010). Plant communities influence decomposition processes directly through litter inputs (Cornwell *et al.,* 2008) and indirectly via their alteration of soil moisture, pH and microbial community composition (Finzi, Canham & Breemen, 1998; Vivanco & Austin 2008). Broadly, rates of decay differ among plant functional types (Zhang *et al*., 2008), with some evidence to support faster rates of plant litter decay in grasslands when compared with forest ecosystems (Solly *et al.,* 2014; Portillo-Estrada *et al.,* 2016). Additionally, decay dynamics can vary within ecosystems depending on the dominant type of mycorrhizal symbiosis that is present. Trees that associate with arbuscular mycorrhizal (AM) fungi often promote soils that have properties distinct from trees that associate with ectomycorrhizal (EM) fungi (Phillips, Brzostek, & Midgley 2013), and such differences can lead to divergent rates of litter decay of the same litters (Midgely, Brzostek, & Phillips 2015; Keller & Phillips 2018). Furthermore, differences in the dominant mycorrhizal symbioses across the landscape often reflect strong gradients in soil pH and nutrient availability (Read & Perez-Mereno, 2003; Phillips *et al.,* 2013; Lin *et al.,* 2017; Jo, Fei, Oswalt, Domke & Phillips, 2019). There is evidence to support that these differences in soil properties may lead to functional variation among decomposer organisms within AM and EM communities (Cheeke *et al.,* 2016: Mushinski *et al*., 2019), creating an ideal testbed for exploring how substrate quality and differences in abiotic and biotic environmental conditions interact to control fungal necromass decay.

Molecular-based identification techniques have led to a rapid increase in the characterization of necromass-associated microbial communities or the 'necrobiome' (Drigo *et al.,* 2012, Brabcová *et al.,* 2016, 2018, Fernandez & Kennedy, 2018, Lopez-Mondejar *et al.,* 2018). Importantly, the composition of the fungal 'necrobiome' has been shown to be distinct from that of the surrounding

soil environment, suggesting that fungal necromass has unique qualities relative to the bulk soil (Brabcová *et al.,* 2016, 2018, Fernandez & Kennedy, 2018). Fungal decomposer communities of necromass are frequently dominated by fast-growing moulds in the order Eurotiales, but also show considerable changes in composition over time (Brabcová *et al.,* 2016, 2018), including significant colonization by EM fungi (Fernandez & Kennedy, 2018). Similarly, bacterial decomposers of fungal necromass appear to be dominated by generalist Proteobacteria, at least initially (Brabcová *et al.,* 2018, Lopez-Mondejar *et al.,* 2018), but also include more specialized taxa such as *Chitinophaga*, which have high chitin degradation abilities (Sangkhobol & Skerman, 1981). Additionally, it appears that necromass quality can significantly influence bacterial and fungal decomposer community composition, either through variation in C:N ratio (Brabcová *et al.,* 2018) or melanin content (Fernandez & Kennedy, 2018).

While there has been notable recent progress in characterizing the effects of abiotic and biotic factors on fungal necromass decomposition and necromass-associated decomposer communities, the generality of the aforementioned patterns remains unclear. This is because all studies of this topic to date have been conducted at single sites. Here, by deploying common fungal necromass substrates in a temperate oak savannah and hardwood forest, we sought to address two key gaps in current knowledge: 1) to determine whether high- and low-quality fungal necromass would decompose differently between the two sites and 2) to characterize the structure of the fungal necromass 'necrobiome' within and across sites under differing vegetation types. We hypothesized that similar to plant litter, high-quality fungal necromass (i.e. low melanin, high N) would decompose more rapidly than low-quality necromass (i.e. high melanin, low N). However, we also predicted that the effects of necromass quality would depend on the dominant vegetation under

which it decayed, with the expectation that plant litter inputs can lead to functional differences in decomposer communities between vegetation types (Lambers, Chapin & Pons 1998 ; Strickland *et al*., 2009). We further hypothesized that both necromass quality and vegetation type would significantly influence the taxonomic and functional guild composition of microbial communities present on decomposing necromass, with fast-growing moulds, yeasts, and copiotrophic bacteria being the dominant decomposers of high-quality necromass and low-quality necromass being more heavily colonized by oligotrophic bacteria as well as saprotrophic and/or EM fungi depending on vegetation type.

Materials and Methods

Study sites

Parallel necromass decomposition experiments were conducted at two sites and under two different vegetation types at each site: a temperate savannah containing EM-associated trees and AM-associated grasses and a temperate hardwood forest containing adjacent EM- and AM-dominated stands. The savannah site was located at Cedar Creek Ecosystem Science Reserve in central Minnesota, USA (N 45.42577 W 093.20852). Cedar Creek is a 2266 ha reserve affiliated with the University of Minnesota, which contains of a mix of prairie and forest ecosystems. The mean annual temperature at Cedar Creek is 6.7°C and the mean annual precipitation is 801 mm. The forest site was located at Moores Creek in south-central Indiana, USA (N 39.08333 W 086.46666). Moores Creek, which is part of the Indiana University Research and Teaching Preserve system, is comprised of 105 ha of mixed deciduous hardwood forest (~80 years in age). The mean annual temperature at Moores Creek is 11.6°C and the mean annual precipitation is 1200

mm. Within both sites, vegetation communities differed in their AM- and EM-associated plant species and edaphic characteristics (Table 1).

Plot locations at each site were chosen based on dominant vegetation type and mycorrhizal association. Three replicate plots were established at two locations in the savannah site; 10 m into EM-dominated *Quercus* forest and 20 m into the adjacent AM-dominated grassland. These distances were chosen based on previous work at the same site by Dickie and Reich (2005), which found little to no EM colonization of *Quercus* seedlings at 20 m away from the forest edge. At the forest site, 7 replicate plots were established based on known mycorrhizal associations of dominant tree species. In all plots, trees from the dominant mycorrhizal type (AM or EM) represented >85% of the basal area of the plot and AM and EM plots were paired according to geographic proximity. Additional details about the layout of the plots in the forest site are available in Midgley and Phillips (2016).

Fungal necromass generation and incubation

Two fungal species, *Mortierella elongata* and *Meliniomyces bicolor*, which have previously been demonstrated to differ in multiple chemical traits (Maillard, Schilling, Andrews, Schreiner, & Kennedy 2020; Table 2), were chosen to represent high- and low-quality necromass. *M. elongata* is a fast-growing saprotrophic fungus in the phylum Mucromycota, which is frequently found in both forest and agricultural soils (Li *et al.*, 2018). *M. bicolor* is an EM and ericoid mycorrhizal (ErM) Ascomycotan fungus frequently found in temperate and boreal forest soils (Grelet, Meharg, Duff, Anderson, Alexander & 2009; see Fehrer, Réblová, Bambasová & Vohník 2019 for an update on the taxonomic status of this genus). These two species have contrasting melanin and

183 nitrogen levels, with *M. elongata* representing a high-quality substrate and *M. bicolor* representing
184 a low-quality substrate (Table 2). Complete details on the methods used for the chemical
185 characterization of both species are provided in the online Supplementary Information.
186
187 Fungal biomass for both species was produced in liquid cultures by individually inoculating 50
188 mL flasks containing half-strength potato dextrose broth with 3 mm diameter mycelial plugs (one
189 plug per flask). Following inoculation, cultures were transferred to an orbital shaker and left to
190 shake at 80 rpm for at least 30 days or until growth stopped. To produce fungal necromass, cultures
191 were rinsed with distilled water and dried at 26°C for 24 hours. Dried fungal necromass (~25 mg)
192 were then placed into nylon mesh litter bags constructed from 53-micron mesh (Elko, Minneapolis,
193 MN, USA) and heat-sealed. The 53-micron mesh size excluded both tree and grass root in-growth.
194 Separate litter bags were constructed for replicates of each fungal species. During deployment,
195 litter bags were buried at organic-mineral soil interface (0-5 cm depth). To determine if there was
196 any mass loss due to transport and handling, an additional set of litter bags was carried into the
197 field (n = 3). Necromass recovery was greater than 98% and did not differ between fungal species,
198 so masses were not corrected for any loss during transport. At each harvest, litter bags were
199 individually bagged, placed on ice, and taken directly to the laboratory for processing. For each
200 sample, necromass was carefully removed from the litterbag and dried at 30°C to a constant mass
201 to determine mass remaining (this temperature was chosen to limit DNA degradation ahead of
202 molecular analyses). Following mass measurements, the remaining necromass was stored at -80ºC
203 for molecular analyses.
204

While the preparation and processing of fungal necromass was standardized across the two sites, the specific incubation times varied slightly between studies due to logistical constraints. At the savannah site, fungal necromass was incubated for 14, 28, 42, and 56 days beginning in July 2017 (n = 3 litter bags of each fungal species for each vegetation type for each sampling date). At the forest site, fungal necromass was incubated for 14, 31, and 92 days beginning in July 2017 (n = 7 litter bags of each fungal species for each vegetation type for each sampling date). Soil moisture measurements at both sites were taken at the time litter bags were harvested. Gravimetric soil moisture data was collected from the composite of two 5 × 10 cm soil cores per plot at the savannah site and three 6.35 × 10 cm soil cores per plot at the forest site. To determine pH, a sub-sample of soil collected at the time of the first litter bag harvest was air-dried and analyzed in a 0.01 M $CaCl_2$ solution using a bench-top pH meter. An additional subsample of soil taken from the first litter bag harvest was stored at -80^{o}C prior to molecular analyses.

Molecular analyses

Total genomic DNA was isolated from soil and necromass samples using DNeasy PowerSoil Extraction Kits (QIAGEN, Germantown, MD, USA). DNA extractions were done according to the manufacturer's instructions, with the addition of a 30 second bead-beating step prior to extraction to enhance sample homogenization (as in Fernandez & Kennedy, 2018). Positive and negative controls were included for both bacteria and fungi. Positive controls included the bacterial mock community from the Human Microbiome Project (https://www.hmpdacc.org/HMMC/) and the fungal synthetic mock community developed by Palmer, Jusino, Banik & Lindner (2018). DNA extractions were also performed on necromass samples that were placed into litterbags but

not incubated. Negative controls included lysis tubes lacking substrate and PCR reactions with no DNA template added.

Microbial communities in soil and on decomposing fungal necromass were identified using high-throughput sequencing (HTS). For bacteria, the 515F-806R primer pair was chosen to target the V4 region of the 16S rRNA gene. For fungi, the 5.8S-Fun and ITS4-Fun primer pair (Taylor *et al.,* 2017) was used to target the ITS2 region of the fungal rRNA operon. Samples were first amplified in individual 20 ul reactions containing 10 ul of Phusion Hot Start II High-Fidelity PCR Master Mix (Thermo Scientific, Waltham, MA, USA), 0.5 ul of each 20 mM primer, 1 ul of DNA template and 8 ul of PCR-grade water. Thermocycling conditions were as follows: 1. 98°C for 30 seconds, 2. 98°C for 10 seconds, 3. 55°C for 30 seconds, 4. 72°C for 30 s, repeat steps 2-4 34 times, 5. 72°C for 10 minutes and 6. infinite hold at 4°C. If initial PCRs were not successful, dilutions or increased cycle numbers (34x) were performed. For all samples with amplicons, a second PCR was run under thermocycling conditions to add unique Golay barcodes and sequencing adaptors. PCR products were then cleaned using the Charm Just-a-Plate Purifiation and Normalization Kit (Charm Biotech, San Diego, CA, USA). Each sample was then pooled at equimolar concentration and sequenced on a full MiSeq lane (2 x 300 bp V3 Illumina chemistry) at the University of Minnesota Genomics Center.

Sequences were processed using the AMPtk pipeline v1.1 (Palmer *et al.*, 2018). First, paired-end reads were merged using VSEARCH (Rognes *et al.,* 2016) and then subjected to quality trimming. Following pre-processing, reads were denoised with UNOISE3 (Edgar, 2016), and clustered into unique OTUs at 97% similarity using USEARCH v10 (Edgar, 2010). A 0.0005 abundance cut-off

was applied to the bacterial data to eliminate low abundance OTUs thought to be spurious. For the fungal data, SynMock abundances were used to determine a similar filtering threshold. Read counts for any OTUs present in PCR and DNA negative controls were also subtracted from all samples. A small number of samples contained OTUs that matched the decomposing necromass (i.e. *M. elongata* and *M. bicolor* necromass). This signal could be residual DNA from the fungal necromass itself or from colonization by closely related species present in the soil. Because we encountered these OTUs in the soils at our sites and previous studies have demonstrated that the DNA associated with necromass decomposes rapidly (~7-14 days, Drigo *et al.,* 2012; Schweigert, Herrmann, Miltner, Fester & Kästner 2015), they were retained in our analyses. However, any bacterial OTUs assigned as chloroplast without genus identification were removed.

Bacterial OTUs were assigned to copiotrophic and oligotrophic tropic modes based on Trivedi *et al.,* (2018). Specifically, all bacterial OTUs belonging to the phylum Bacteroidetes and classes alpha-Proteobacteria, beta-Proteobacteria and gamma-Proteobacteria were defined as copiotrophs, while bacterial OTUs belonging to phylum Acidobacteria and class delta-Proteobacteria were defined as oligotrophs. Trophic mode assignments for fungi were made with FUNGuild (Nguyen *et al.,* 2016). Fungi that could not be assigned to a functional guild were classified as "unidentified." Symbiotrophic fungi were parsed between ectomycorrhizal fungi and arbuscular mycorrhizal fungi. Remaining fungal OTUs belonging to Eurotiales, Hypocreales, Morteriellales, Mucorales, Saccharomycetales, Tremellales and Sporidiales as well as fungal OTUs defined by FUNGuild as microfungi, yeast and facultative yeast were classified as moulds and yeasts, following Sterkenburg *et al.* (2015).

Statistical analyses

Statistical analyses and data visualization were conducted in R version 3.5.1 (R Core Team, 2018). Analysis of variance (ANOVA) was used to test for differences in soil pH between sites and vegetation types within sites. To test for differences in soil moisture, ANOVAs were run with vegetation type (AM- vs. EM-associated vegetation) and sampling date as the predictor variables for each site. Prior to running the ANOVAs, soil moisture data was log-transformed to meet the assumptions of normality. Linear mixed-effect (LME) models were used to analyze the amount of fungal necromass remaining within each site (Bradford, Berg, Maynard, Wieder & Wood 2016). Fixed predictor factors included vegetation type (AM- vs. EM-associated vegetation), necromass type (high- vs. low-quality), incubation period, and soil moisture. Replicate sampling locations (either plots or plot pairs) were designated as a random factor. Because pH was only measured during one harvest at each site it was not included in this analysis. Mass remaining data were log logit-transformed to meet statistical assumptions (Sokal & Rohlf, 1995; Warton & Hui, 2011). To evaluate the significance of linear mixed-effects models the Kenward-Roger approximation was used to estimate F statistics and denominator degrees of freedom (Halekoh & Højsgaard, 2014). Least square means were computed for each fixed effect and post-hoc comparisons were carried out on pairs of the least-squares means using the Tukey's adjustment for multiple comparisons.

Given the well-established non-linear nature of OM decomposition (Berg, 2014), decay constants were calculated separately for each necromass type at each site. To calculate decay constants, we fit the proportion of remaining necromass against incubation time (days) using single- and double-exponential decay models. The best fitting model was selected using Akaike's Information Criteria (AIC). According to AIC values, a double-exponential decay model (Equation1) produced the best fit.

Equation 1: $[mass]_t = ae^{-k_1 t} + (1-a)\, e^{-k_2 t}$

The proportional mass remaining ($[mass]_t$) was calculated by dividing the mass remaining at time (t) by the initial mass for each litterbag. In equation 1, a refers to is the initial proportion of fast decomposing or labile material, 1-a is the initial proportion of slow decomposing or recalcitrant material. k_1 and k_2 are the degradation rate constants of the labile (fast-decomposing) and recalcitrant (slow-decomposing pool), respectively. The nonlinear least-squares Levenberg-Marquardt algorithm used to estimate model parameters, a, k_1 and k_2, using the 'minpak.lm' package (Elzhov, Mullen, Spiess & Bolker 2016). Like the mass remaining analyses, due to differences in the fungal necromass incubation times at the two sites, the following microbial community analyses were analyzed for each site separately. Sample-OTU accumulation curves indicated that most samples achieved sequencing depths with high levels of OTU saturation (Fig. S1). To account for differences in sequence read totals among samples, rarefaction was applied to 4000 and 1000 reads/sample for bacteria and fungi, respectively. OTU richness (N0) and diversity (H) were calculated using the 'vegan' package (Oksanen *et al.,* 2013). The effect of vegetation type, necromass quality, and incubation period on each of these metrics was assessed using a series of three-way ANOVAs for each decomposer group (bacteria or fungi) separately. Due to successful sequencing of only one 56-day sample at the savannah site, that harvest date was not included in the ANOVAs. Additionally, to balance the sampling design between sites (i.e. each site having an equal number samples from AM and EM vegetation types), all of the samples from the 5m grassland plots in the savannah site were not included in the ANOVAs, as preliminary analyses revealed very similar patterns of richness and diversity between the two AM grass-dominated plots (data not shown). Prior to running each ANOVA, variance homoscedasticity was tested using Cochran's test and data were log-transformed if necessary.

For analyses of microbial community composition, quality-filtered sequence read counts were transformed to proportional data per sample for all bacterial and fungal OTUs. Differences in bacterial and fungal OTU composition were visualized with non-metric multi-dimensional scaling (NMDS) plots using the 'metaMDS' function. The NMDS plots were generated based on Bray-Curtis OTU dissimilarity matrices. Permutational multivariate analyses of variance (PERMANOVA) were applied to assess the effect of vegetation type, necromass quality, and incubation period on microbial community composition. Effects of the same three predictor variables were also assessed for each microbial guild using three-way ANOVAs. Finally, Wilcoxon signed-rank tests were used to identify specific bacterial and fungal genera that had significantly differential relative abundance depending on necromass quality. Similar to the analyses of richness and diversity, preliminary analyses of two AM grass-dominated plots at the savannah site revealed very high similarity in OTU and guild composition, so all samples from the 5 m grassland plots were not included in any of the community composition analyses. All tests were considered significant using a threshold of $P \leq 0.05$.

Results

Soil pH did not differ between sites ($F_{1,19} = 1.20$, $P = 0.291$), but did differ between vegetation types within sites ($F_{1,19} = 5.17$, $P = 0.038$), being ~1 pH unit lower under EM vegetation compared to soils under AM vegetation (Table 1). In contrast to pH, soil moisture did not differ between vegetation types ($F_{1,57} = 0.010$, $P = 0.921$), but there was a modest difference between sites ($F_{1,57} = 3.96$, $P = 0.051$). On average, the savannah site soils were ~65% wetter (10.6 ± 0.5%) (mean ±

342 1 s.e.) during the necromass decay period than those at the forest site (6.8 ± 0.4%) over the duration
343 of the incubations.
344
345 At each site, the amount of mass remaining in fungal necromass was significantly influenced by
346 both necromass quality ($F_{1,37}$ = 20.24, and $F_{1,66}$ = 100.22 for the savannah and forest sites
347 respectively; P values < 0.001) and incubation period (savannah, $F_{1,37}$ = 74.29; forest, $F_{1,66}$ =
348 66.76; P values < 0.001), but not vegetation type (savannah, $F_{1,37}$ = 0.24, P = 0.627; forest, $F_{1,66}$
349 = 0.26, P = 0.609). On average, the high-quality fungal necromass decomposed 2-3 times faster
350 than low-quality fungal necromass. However, the effect of necromass quality was mediated by
351 incubation time (see quality by time interaction terms in Table S1), with the greatest differences
352 between quality types occurring at 14-days (Fig. 1). After 14 days, 60% and 80% more low-quality
353 necromass remained at the savannah and forest sites respectively, but after 56 and 92 days, the
354 mass remaining of both necromass types reached a similarly stable value (~80% mass loss; Fig.
355 1). No other higher order interactions were significant (Table S1). The non-linear decay models
356 showed similar trends, with k_1 values being much higher at both sites for high-quality fungal
357 necromass, and the k_2 values being largely equivalent across sites and necromass types (Fig. 1 &
358 Fig. S1).
359
360 Microbial OTU diversity was significantly higher under AM- than EM-dominated vegetation soils,
361 particularly fungal communities at the savannah site and bacterial communities at the forest site
362 (Fig. 2a,b, Table S2). Bacterial OTU diversity was ~50% lower on necromass than in the
363 surrounding soil at both sites (Fig. 2c) and fungal OTU diversity was also decreased on necromass
364 relative to soil, although only significantly at the savannah site (Fig. 2d). Microbial diversity was

20% higher, on average, on high than low quality necromass, being significant at the forest site for bacteria and both sites for fungi (Fig. 2e,f). The effect of vegetation type on microbial OTU diversity was generally low, only being significantly higher for fungi in AM vegetation at the forest site (Fig. 2g,h). Similarly, incubation period had a limited impact on microbial OTU diversity, only being significantly higher for bacteria after 92 days of incubation at the forest site (Fig. 2i,j).

Like OTU diversity, the composition of bacterial and fungal communities in soil and on necromass was significantly different at both sites (Fig. 3, Table S4). Soils under EM vegetation were dominated by EM fungi and oligotrophic bacteria, whereas soils under AM vegetation had some AM fungi, but a greater proportion of saprotophic fungi along with oligotrophic bacteria (Fig. 4 & Fig. S6). By contrast, yeasts, moulds, and copiotrophic bacteria were much more common on necromass at both sites (Fig. 4). Necromass quality significantly influenced bacterial composition at both sites and fungal community composition at the forest site (Table S5). In general, high-quality fungal necromass had greater relative abundances of copiotrophic bacteria, moulds, yeasts, and less saprotrophic fungi (Fig. S7). Microbial community composition was also significantly influenced by vegetation type (Table S5), with fungal pathotrophs being more abundant on fungal necromass in AM-dominated vegetation and EM and AM fungi being more abundant on fungal necromass in their matching vegetation types, respectively (Fig. 4). Additionally, incubation time significantly affected bacterial but not fungal community composition on fungal necromass at both sites (Table S5), with oligotrophic bacteria increasing in abundance over time at both sites, particularly on low-quality fungal necromass at the forest site (Fig. 4, Table S5).

A number of bacterial and fungal genera displayed significant differential abundances depending on necromass quality. Both across sites (i.e. savannah v. forest) and between vegetation types (AM v. EM vegetation), the bacterial genera most commonly detected in greater abundance on high-quality fungal necromass included *Nocardia*, *Mesorhizobium*, *Orchobactrum*, and *Chitinophaga* (Fig. 5). In contrast, the bacterial genera most commonly found in greater abundance on low-quality fungal necromass included *Burkholderia* and *Mucilaginibacter*. Of the fungal genera that had significant differential abundance by necromass quality, *Mortierella* was the lone genus consistently found on high-quality fungal necromass within and across both sites, although *Mucor* and *Pochonia* showed similar preferences for high-quality fungal necromass (Fig. 6). Fungal genera most positively associated with low-quality fungal necromass included *Talaromyces* at both sites, *Clonostachys* at the forest site, and *Chaetosphaeria* at the savannah site.

Discussion

In this study, we utilized differences between study systems and vegetation types to explore the relative importance of necromass quality and edaphic characteristics in controlling fungal necromass decay and microbial decomposer community structure. We found that the effects of necromass quality on decay were robust to vegetation type as well as differences in site edaphic characteristics. High-quality fungal necromass decomposed, on average, 2.5 times faster during the initial stages of decay regardless of site-level variation in soil moisture, pH, or CDI. This result is consistent with recent studies that have found substrate quality to be a key local predictor of fungal necromass decay. Brabcová *et al.* (2018) demonstrated that decreasing C:N ratio was positively associated with increasing mass loss rates from dead mycelium of 12 fungal species.

Likewise, Fernandez and Kennedy (2018) showed at differences in substrate quality, particularly increased melanin content, were strongly associated with decreases in mass loss rates. Collectively, these results indicate that, like plant litter decay, substrate quality is a key driver of fungal decay at both local and regional scales.

We did not find support for our hypothesis that necromass quality would interact with vegetation type to determine decay rate. This was somewhat surprising, particularly at the temperate forest site, given that the mycorrhizal associations of dominant tree species at this site have been shown to have distinct effects on soil biogeochemistry via their selection of microbial groups (including mycorrhizal fungi) with differing enzyme function (Midgley, Brzostek & Phillips 2015; Brzostek, Dragoni, Brown & Phillips 2015; Rosling *et al.,* 2016; Cheeke *et al.,* 2016; Lin *et al.,* 2017). We speculate that the difference between our results and those of previous studies may be due to the fact that fungal necromass used in this study had chemical qualities that would be considered high compared to plant litter. Specifically, the C:N ratios for the two necromass types was 7 and 13 respectively, which is much lower than C:N ratios typically reported for leaf litter which can range from 20-100 (Zhang *et al.,* 2008; Ferlian, Wirth & Eisenhauer 2017; Brabcová *et al.,* 2018). In this case, the higher nutrient content of fungal necromass may not demand the same selective enzymatic activity to facilitate decomposition, particularly if initial rates of mass loss are influenced by differences in leaching capacity rather direct microbial degradation (Maillard *et al.,* 2020). It is certainly possible that with more time, differences in the decomposition of the more recalcitrant fraction of the remaining fungal necromass would develop between vegetation types, though the rapid mass loss from our high-quality necromass is consistent with a similarly fast rate of mass loss recently observed for AM necromass in temperate AM-dominated forests in Japan

(Schäfer, Dannoura, Ataka & Osawa 2019). Moreover, given that hyphal production can be 2-3-fold greater in EM-dominated plots relative to AM-dominated plots (Cheeke *et al.,* unpublished data), total inputs of C and N from necromass may depend on vegetation types.

The overall patterns of microbial community diversity on decaying fungal necromass were notably similar between sites, necromass qualities, vegetation types, and incubation times. The lower richness of bacterial and fungal communities on fungal necromass relative to bulk soil likely reflects the active growth required to colonize new substrates, which unlike soil, may contain little 'relic' DNA (Carini *et al.,* 2016). The greater microbial diversity on high-quality necromass relative to low quality necromass suggests that this resource is utilized by a wider variety of microbes like fungi, which had elevated diversity on high-quality necromass at both sites. While the diversity of microbial communities was higher under AM- than EM-dominated vegetation, diversity on necromass was equivalent between vegetation types. The commonality of this finding suggests that fungal necromass may foster a distinct community of decomposers, likely due to its unique chemical composition (Brabcová *et al.,* 2018; Lopez-Mondejar *et al.*, 2018). Further, the general absence of an incubation time effect on microbial diversity indicates that fungal necromass likely represents a sustained 'hotspot' of decomposition (*sensu* Brabcová *et al.,* 2016), even after the rapid mass loss observed during the first weeks of incubation. The general equivalency in microbial community diversity over time appears to be due to substitutions rather than gains or losses in local OTU dominance, likely reflecting shifts in substrate chemistry and the availability of resources during the course of necromass decomposition (Drigo *et al.,* 2012; Tláskal, Voříšková, & Baldrian 2016; Certano, Fernandez, Heckman & Kennedy 2018, Fernandez, Heckman, Kolka, & Kennedy 2019; Ryan *et al*., in press).

Analyses of the microbial guilds colonizing the different types of fungal necromass were also notably similar across sites. At both the savannah and forest sites, fast-growing moulds and copiotrophic bacteria dominated the necrobiome, particularly during early stages of decay. Generalist fungal saprotrophs were also a common part of the necrobiome, although their relative abundances were frequently negatively correlated with fungal pathotroph relative abundance. We suggest the latter guild-level pattern may the direct result of mycoparasitism rather than generalist fungal pathogen accumulation. Specifically, the high relative abundance of the fungal genus *Clonostachys*, which has been demonstrated to be an effective fungal biocontrol agent (Cota, Maffia, Mizubuti & Macedo 2008), indicates that the rapid increase in living fungi on decomposing mycelium, may itself be a target for resource exploitation. Furthermore, when grouped at the genus level, differences in relative abundances of many bacteria and fungi between the two necromass types aligned with their putative decomposition preferences and abilities. For example, many chitinolytic bacteria (e.g. *Chitinophaga* (Sangkhobol & Skerman 1981), *Stretrophonas* (Yoon, Kang, Oh & Oh 2006), *Variovax* (Bers *et al.*, 2011) and fungi (*Mortierella*: De Boer, Gerards, Klein, Gunnewiek & Modderman 1999) had significantly higher abundance on the high-quality fungal necromass, which may reflect easier access to chitin not imbedded in a melanized cell wall matrix (Bull, 1970). Conversely, the higher abundance of bacterial genera such as *Mucilinibacter* and *Granulicella* as well as fungal genera such as *Chaetosphaeria* and *Talaromyces* on low-quality necromass is consistent with their common association with decomposing leaf litter and wood (Huhndorf & Fernandez, 2001, Pankratov, Ivanova, Dedysh & Liesack 2011, Lopez-Mondejar *et al.*, 2016, Yilmaz *et al.*, 2016), which requires greater carbohydrate-active enzymes activity to initiate decomposition. Additionally, the high overlap in

479 the dominant microbial genera detected on fungal necromass at both our study sites and those
480 present on fungal necromass in other study systems (Brabcova *et al.,* 2016, 2018, Lopez-Mondejar
481 *et al.*, 2018, Fernandez & Kennedy, 2018), suggests there may be core necrobiome (Shade &
482 Handelsmann, 2012) that is broadly associated with decomposing mycelium.
483
484 While our results provide novel insights into the dynamics of fungal necromass decomposition,
485 there are some methodological caveats that warrant mentioning. In particular, our two necromass
486 substrates differed in multiple aspects of their initial biochemistry, including both melanin and
487 nitrogen. As noted above, it is likely that these two traits interact to determine the quality of fungal
488 necromass for decomposers (Fernandez & Koide, 2014); as such, future tests should disentangle
489 the relative importance of each to necromass decay rates. Given the recent documentation of fungal
490 necromass C being disproportionately utilized by bacteria relative to fungi (Lopez-Mondejar *et*
491 *al.,* 2018), but also the significant C and N mining from fungal necromass by EM fungi (Akroume
492 *et al.,* 2019), it will also be important to use isotopic labeling techniques to understand exactly
493 which resources are utilized by which microorganisms, particularly in field settings where
494 symbiotic fungi are present (Zeglin, Kluber, & Myrold 2013; Fernandez & Kennedy, 2018;
495 Maillard *et al.,* 2020). Additionally, like most studies of microbial communities, we relied on
496 relative sequence read counts as a proxies for microbial community abundances. There are known
497 issues with this approach in terms of potential taxonomic biases (Lloyd-Macgilp *et al.,* 1996, but
498 see Lekberg & Helgason 2018) as well as count differences being affected by variation in gene
499 copy number (Lofgren *et al.,* 2019). As such, the differential relative abundances we observed
500 across our experimental treatments must be interpreted with some caution. However, the notable
501 consistency in effects of necromass quality across study systems as well as differential responses

of fungi to vegetation type and bacteria to incubation period suggest that our results did capture significant ecological signal. Lastly, we recognize the limitations of the litter-bag technique, which excludes potentially important decomposers including soil fauna, as well as roots and rhizosphere-associated microbes (Bradford, Tordoff, Eggers, Jones & Newington 2002; Crowther *et al.*, 2013; Brzostek *et al.,* 2015).

Conclusions

In this study we demonstrate the regional-scale importance of fungal necromass quality in influencing both decay rate and microbial community composition across sites differing in their edaphic characteristics and vegetation types. Our results contribute to a growing body of literature that recognizes the importance of fungal necromass as a fast cycling OM resource that supports a distinct assemblage of decomposers with consistent taxonomic and functional guild membership. Future studies analyzing the community structure of fungal necromass-associated microbial communities in tropical ecosystems will be particularly valuable in gaining a global perspective on the consistency of the fungal 'necrobiome'. While our work emphasizes the link between substrate quality and decomposer community structure, additional studies are required to link specific characteristics of fungal necromass quality and the necrobiome to long-term soil C stabilization.

Acknowledgements

We thank Christopher Fernandez and Craig See for their input during project conceptualization. We would also like to thank Jeff White for providing lab space to perform DNA extractions, Megan Midgley for establishing the plots at Moores Creek, Amanda Certano for preparing the

HTS library, and Katie Scheiner for assistance with necromass chemical characterization. We are grateful to the members of the Kennedy and Phillips labs for their feedback as well as the constructive suggestions of two anonymous reviewers for on earlier drafts of this manuscript. Funding for this work was provided by the U.S. Department of Energy Office of Biological and Environmental Research, Terrestrial Ecosystem Science Program (Award# DE-SC0016188) to RPP and University of Minnesota Undergraduate Research Opportunity Program grant EA.

Authors' Contributions

K.V.B designed and performed the experiment at Moores Creek, collected data, analyzed data, and co-wrote the manuscript. R.P.P contributed to experimental design and manuscript preparation. E.A. generated the necromass, performed the experiment at Cedar Creek, collected data and contributed to the final version of the manuscript. F.M. performed analyses of microbial community data and contributed to manuscript preparation. R.M.M assisted with DNA extractions and contributed to manuscript preparation. P.G.K. conceived of and designed the study, supervised the research, and co-wrote the manuscript.

Data availability

Raw .fastq files for all samples are available under the following NCBI BioProject Accessions: Moores Creek Bacteria (PRJNA607032), Moores Creek Fungi (PRJNA607029), Cedar Creek Bacteria (PRJNA607034), Cedar Creek Fungi (PRJNA607030). Fungal necromass remaining, pH,

and soil moisture data for both sites can be accessed through the Dryad Digital Repository: https://doi.org/10.5061/dryad.nk98sf7qj (Beidler *et al.* 2020).

References

Adair, E. C., Parton, W. J., Del Grosso, S. J., Silver, W. L., Harmon, M. E., Hall, S. A., … Hart, S. C. (2008). Simple three-pool model accurately describes patterns of long-term litter decomposition in diverse climates. *Global Change Biology*. *14*(11), 2636–2660. doi: 10.1111/j.1365-2486.2008.01674.x

Allen, M. F., & Kitajima, K. (2014). Net primary production of ectomycorrhizas in a California forest. *Fungal Ecology*, *10*(1), 81–90. doi: 10.1016/j.funeco.2014.01.007

Baskaran, P., Hyvönen, R., Berglund, S. L., Clemmensen, K. E., Oran, G., Agren, I., … Manzoni, S. (2017). Modelling the influence of ectomycorrhizal decomposition on plant nutrition and soil carbon sequestration in boreal forest ecosystems. *New Phytologist*, *213*(3), 1452-1465. doi: 10.1111/nph.14213

Beidler, K.V., Phillips, R.P, Andrews, E., Maillard, F., Mushinski, R.M., & Kennedy, P.G. (2020). Data from: Substrate quality drives fungal necromass decay and decomposer community structure under contrasting vegetation types. Dryad Digital Repository. https://doi.org/10.5061/dryad.nk98sf7qj

Berg, B. (2014). Decomposition patterns for foliar litter - A theory for influencing factors. *Soil Biology and Biochemistry*, 78, 222–232. doi: 10.1016/j.soilbio.2014.08.005

Berg, B., & McClaugherty, C. (2003). *Plant Litter:Decomposition, Humus Formation, Carbon Sequestration*. Heidelberg, NY: Springer-Verlag. doi: 10.1007/978-3-642-38821-7

Bers, K., Leroy, B., Breugelmans, P., Albers, P., Lavigne, R., Sørensen, S. R., … Springael, D. (2011). A novel hydrolase identified by genomic-proteomic analysis of phenylurea herbicide mineralization by Variovorax sp. strain SRS16. *Applied and Environmental Microbiology*, *77*(24), 8754–8764. doi: 10.1128/AEM.06162-11

Brabcová, V., Nováková, M., Davidová, A., & Baldrian, P. (2016). Dead fungal mycelium in forest soil represents a decomposition hotspot and a habitat for a specific microbial community. *New Phytologist*, *210*(4), 1369–1381. doi: 10.1111/nph.13849

Brabcová, V., Štursová, M., & Baldrian, P. (2018). Nutrient content affects the turnover of fungal biomass in forest topsoil and the composition of associated microbial communities. *Soil Biology and Biochemistry*, *118*, 187–198. doi: 10.1016/j.soilbio.2017.12.012

579 Bradford, M. A., Berg, B., Maynard, D. S., Wieder, W. R., & Wood, S. A. (2016).
580 Understanding the dominant controls on litter decomposition. *Journal of Ecology*, *104*(1),
581 229–238. doi: 10.1111/1365-2745.12507

582 Bradford, M. A., Tordoff, G. M., Eggers, T., Jones, T. H., & Newington, J. E. (2002).
583 Microbiota, fauna, and mesh size interactions in litter decomposition. *Oikos*, *99*(2), 317–
584 323. doi: 10.1034/j.1600-0706.2002.990212.x

585 Bray, J. R., & Gorham, E. (1964). Litter Production in Forests of the World. *Advances in*
586 *Ecological Research*, *2*, 101-156. doi: 10.1016/S0065-2504(08)60331-1

587 Brzostek, E. R., Dragoni, D., Brown, Z. A., & Phillips, R. P. (2015). Mycorrhizal type
588 determines the magnitude and direction of root-induced changes in decomposition in a
589 temperate forest. *New Phytologist*, *206*(4), 1274–1282. doi: 10.1111/nph.13303

590 Bull, A. T. (1970). Inhibition of polysaccharases by melanin: Enzyme inhibition in relation to
591 mycolysis. *Archives of Biochemistry and Biophysics*, *137*(2), 345–356. doi: 10.1016/0003-
592 9861(70)90448-0

593 Carini, P., Marsden, P. J., Leff, J. W., Morgan, E. E., Strickland, M. S., & Fierer, N. (2016).
594 Relic DNA is abundant in soil and obscures estimates of soil microbial diversity. *Nature*
595 *Microbiology*, *2*, 16242. doi: 10.1038/nmicrobiol.2016.242

596 Certano, A. K., Fernandez, C. W., Heckman, K. A., & Kennedy, P. G. (2018). The afterlife
597 effects of fungal morphology: Contrasting decomposition rates between diffuse and
598 rhizomorphic necromass. *Soil Biology and Biochemistry*, *126*, 76–81. doi:
599 10.1016/j.soilbio.2018.08.002

600 Chapin S., F., Matson, P. A., & Vitousek, P. M. (2012). Principles of terrestrial ecosystem
601 ecology. In *Principles of Terrestrial Ecosystem Ecology*. doi: 10.1007/978-1-4419-9504-9

602 Cheeke, T. E., Phillips, R. P., Brzostek, E. R., Rosling, A., Bever, J. D., & Fransson, P. (2016).
603 Dominant mycorrhizal association of trees alters carbon and nutrient cycling by selecting
604 for microbial groups with distinct enzyme function. *New Phytologist*, *214*(1), 432-442. doi:
605 10.1111/nph.14343

606 Cheeke, T.E., Phillips, R.P., Kuhn, A., Rosling, A., Fransson, P. (2019).Variation in mycorrhizal
607 hyphal production rather than turnover regulates standing fungal biomass in temperate
608 hardwood forests. Unpublished data.

609 Clemmensen, K. E., Bahr, A., Ovaskainen, O., Dahlberg, A., Ekblad, A., Wallander, H., …
610 Lindahl, B. D. (2013). Roots and associated fungi drive long-term carbon sequestration in
611 boreal forest. *Science*, *339*(6127), 1615–1618. doi: 10.1126/science.1231923

612 Cleveland, C. C., Reed, S. C., Keller, A. B., Nemergut, D. R., O'Neill, S. P., Ostertag, R., &
613 Vitousek, P. M. (2014). Litter quality versus soil microbial community controls over

614 decomposition: A quantitative analysis. *Oecologia*, *174*(1), 283–294. doi: 10.1007/s00442-
615 013-2758-9

616 Cornwell, W. K., Cornelissen, J. H. C., Amatangelo, K., Dorrepaal, E., Eviner, V. T., Godoy, O.,
617 … Westoby, M. (2008). Plant species traits are the predominant control on litter
618 decomposition rates within biomes worldwide. *Ecology Letters*, *11*(10), 1065–1071. doi:
619 10.1111/j.1461-0248.2008.01219.x

620 Cota, L. V., Maffia, L. A., Mizubuti, E. S. G., & Macedo, P. E. F. (2009). Biological control by
621 Clonostachys rosea as a key component in the integrated management of strawberry gray
622 mold. *Biological Control*, *50*(3), 222–230. doi: 10.1016/j.biocontrol.2009.04.017

623 Crowther, T. W., Stanton, D. W. G., Thomas, S. M., A'Bear, A. D., Hiscox, J., Jones, T. H., …
624 Boddy, L. (2013). Top-down control of soil fungal community composition by a globally
625 distributed keystone consumer. *Ecology*, *94*(11), 2518–2528. doi: 10.1890/13-0197.1

626 De Boer, W., Gerards, S., Klein Gunnewiek, P. J. A., & Modderman, R. (1999). Response of the
627 chitinolytic microbial community to chitin amendments of dune soils. *Biology and Fertility*
628 *of Soils*, *29*(2), 170–177. doi: 10.1007/s003740050541

629 Dickie, I. A., & Reich, P. B. (2005). Ectomycorrhizal fungal communities at forest edges.
630 *Journal of Ecology*. doi: 10.1111/j.1365-2745.2005.00977.x

631 Drigo, B., Anderson, I. C., Kannangara, G. S. K., Cairney, J. W. G., & Johnson, D. (2012).
632 Rapid incorporation of carbon from ectomycorrhizal mycelial necromass into soil fungal
633 communities. *Soil Biology and Biochemistry*, *49*, 4–19. doi: 10.1016/j.soilbio.2012.02.003

634 Edgar, R. C. (2016). UNOISE2: improved error-correction for Illumina 16S and ITS amplicon
635 sequencing. In *bioRxiv*. doi: 10.1101/081257

636 Edgar, R. C. (2010). Search and clustering orders of magnitude faster than BLAST.
637 *Bioinformatics*, 2460–2461. doi: 10.1093/bioinformatics/btq461

638 Ekblad, A., Wallander, H., Godbold, D. L., Cruz, C., Johnson, D., Baldrian, P., … Plassard, C.
639 (2013). The production and turnover of extramatrical mycelium of ectomycorrhizal fungi in
640 forest soils: Role in carbon cycling. *Plant and Soil*, pp. 1–27. doi: 10.1007/s11104-013-
641 1630-3

642 Ekblad, A., Wallander, H., & Näsholm, T. (1998). Chitin and ergosterol combined to measure
643 total and living fungal biomass in ectomycorrhizas. *New Phytologist*, *138*(1), 143–149. doi:
644 10.1046/j.1469-8137.1998.00891.x

645 Elzhov, T., Mullen, K., Spiess, A., & Bolker, B. (2016). Package "minpack. lm." In
646 *Https://Cran.R-Project.Org/Web/Packages/Minpack.Lm/Minpack.Lm.Pdf*.

Eviner, V.T., & Chapin, F.S. (2003). Biogeochemical interactions and biodiversity. In: Melillo JM., Field, CB, Moldan, M (Eds.) Element interactions: rapid assessment project of SCOPE (pp.151-173). Washington: Island Press.

Fehrer, J., Réblová, M., Bambasová, V., & Vohník, M. (2019). The root-symbiotic Rhizoscyphus ericae aggregate and Hyaloscypha (Leotiomycetes) are congeneric: Phylogenetic and experimental evidence. *Studies in Mycology*, *92*, 195–225. doi: 10.1016/j.simyco.2018.10.004

Ferlian, O., Wirth, C., & Eisenhauer, N. (2017). Leaf and root C-to-N ratios are poor predictors of soil microbial biomass C and respiration across 32 tree species. *Pedobiologia*, *25*, 16-23. doi: 10.1016/j.pedobi.2017.06.005

Fernandez, C. H. W. F., & Koide, R. T. (2012). The role of chitin in the decomposition of ectomycorrhizal fungal litter. *Ecology*, *93*(1), 24–28.

Fernandez, C. W., Heckman, K., Kolka, R., & Kennedy, P. G. (2019). Melanin mitigates the accelerated decay of mycorrhizal necromass with peatland warming. *Ecology Letters*, Vol. 22, pp. 498–505. doi: 10.1111/ele.13209

Fernandez, C. W., & Kennedy, P. G. (2018). Melanization of mycorrhizal fungal necromass structures microbial decomposer communities. *Journal of Ecology*, *106*(2), 468–479. doi: 10.1111/1365-2745.12920

Fernandez, C. W., Langley, J. A., Chapman, S., McCormack, M. L., & Koide, R. T. (2016). The decomposition of ectomycorrhizal fungal necromass. *Soil Biology and Biochemistry*, Vol. 93, pp. 38–49. doi: 10.1016/j.soilbio.2015.10.017

Fernandez, C. W., & Koide, R. T. (2014). Initial melanin and nitrogen concentrations control the decomposition of ectomycorrhizal fungal litter. *Soil Biology and Biochemistry*, *77*, 150–157. doi: 10.1016/j.soilbio.2014.06.026

Fernandez, C. W., See, C. R., & Kennedy, P. G. (2019). Decelerated carbon cycling by ectomycorrhizal fungi is controlled by substrate quality and community composition. *BioRxiv*, 716555. doi: 10.1101/716555

Finlay, R. D., & Clemmensen, K. E. (2016). Immobilization of Carbon in Mycorrhizal Mycelial Biomass and Secretions. In: Johnson, NC, Gehring, CA & Jansa, J (Eds.). Mycorrhizal Mediation of Soil: Fertility, Structure, and Carbon Storage (pp. 413-440). Cambridge, MA: Elsevier.doi: 10.1016/B978-0-12-804312-7.00023-1

Finzi, A. C., Canham, C. D., & Van Breemen, N. (1998). Canopy tree-soil interactions within temperate forests: Species effects on pH and cations. *Ecological Applications*, *8*(2), 447–454. doi: 10.1890/1051-0761(1998)008[0447:CTSIWT]2.0.CO;2

Godbold, D. L., Hoosbeek, M. R., Lukac, M., Cotrufo, M. F., Janssens, I. A., Ceulemans, R., … Peressotti, A. (2006). Mycorrhizal hyphal turnover as a dominant process for carbon input into soil organic matter. *Plant and Soil*, *281*(1–2), 15–24. doi: 10.1007/s11104-005-3701-6

Grelet, G. A., Meharg, A. A., Duff, E. I., Anderson, I. C., & Alexander, I. J. (2009). Small genetic differences between ericoid mycorrhizal fungi affect nitrogen uptake by Vaccinium. *New Phytologist*, *18*(3), 708–718. doi: 10.1111/j.1469-8137.2008.02678.x

Halekoh, U., & Højsgaard, S. (2014). A kenward-Roger approximation and parametric bootstrap methods for tests in linear mixed models-the R package pbkrtest. *Journal of Statistical Software*, *59*(9), 1–30.

Hooper, D. U., & Vitousek, P. M. (1997). The effects of plant composition and diversity on ecosystem processes. *Science*, *277*(5330), 1302–1305. doi: 10.1126/science.277.5330.1302

Huhndorf, S. M., Fernández, F. A., Taylor, J. E., & Hyded, K. D. (2001). Two pantropical Ascomycetes: Chaetosphaeria cylindrospora sp. nov. and Rimaconus, a new genus for Lasiosphaeria jamaicensis. *Mycologia*, *93*(6), 1072–1080. doi: 10.2307/3761669

Hurst, H. M., & Wagner, G. H. (1969). Decomposition of 14C-Labeled Cell Wall and Cytoplasmic Fractions from Hyaline and Melanic Fungi. *Soil Science Society of America Journal*, *33*(5), 707–711. doi: 10.2136/sssaj1969.03615995003300050025x

Jo, I., Fei, S., Oswalt, C. M., Domke, G. M., & Phillips, R. P. (2019). Shifts in dominant tree mycorrhizal associations in response to anthropogenic impacts. *Science Advances*, *5.4*, eaav6358. doi: 10.1126/sciadv.aav6358

Keller, A. B., & Phillips, R. P. (2019). Leaf litter decay rates differ between mycorrhizal groups in temperate, but not tropical, forests. *New Phytologist*, *222*(1), 556–564. doi: 10.1111/nph.15524

Koide, R. T., & Malcolm, G. M. (2009). N concentration controls decomposition rates of different strains of ectomycorrhizal fungi. *Fungal Ecology*, *2*(4), 197–202. doi: 10.1016/j.funeco.2009.06.001

Lambers, H., Chapin, F.S., Pons, T.L.(1998). Plant physiological ecology. New York, NY: Springer-Verlag.

Lekberg, Y., & Helgason, T. (2018). In situ mycorrhizal function – knowledge gaps and future directions. *New Phytologist*, *220*(4), 957–962. doi: 10.1111/nph.15064

Lenaers, M., Reyns, W., Czech, J., Carleer, R., Basak, I., Deferme, W., … Rineau, F. (2018). Links Between Heathland Fungal Biomass Mineralization, Melanization, and Hydrophobicity. *Microbial Ecology*, *76*(3), 762–770. doi: 10.1007/s00248-018-1167-3

Li, F., Chen, L., Redmile-Gordon, M., Zhang, J., Zhang, C., Ning, Q., & Li, W. (2018). Mortierella elongata's roles in organic agriculture and crop growth promotion in a mineral soil. *Land Degradation and Development*, *29*(6), 1642–1651. doi: 10.1002/ldr.2965

Lin, G., McCormack, M. L., Ma, C., & Guo, D. (2017). Similar below-ground carbon cycling dynamics but contrasting modes of nitrogen cycling between arbuscular mycorrhizal and ectomycorrhizal forests. *New Phytologist*, *213*(3), 1440–1451. doi: 10.1111/nph.14206

Lloyd-Macgilp, S. A., Chambers, S. M., Dodd, J. C., Fitter, A. H., Walker, C., & Young, J. P. W. (1996). Diversity of the ribosomal internal transcribed spacers within and among isolates of Glomus mosseae and related mycorrhizal fungi. *New Phytologist*, *133*(1), 103–111. doi: 10.1111/j.1469-8137.1996.tb04346.x

Lofgren, L. A., Uehling, J. K., Branco, S., Bruns, T. D., Martin, F., & Kennedy, P. G. (2019). Genome-based estimates of fungal rDNA copy number variation across phylogenetic scales and ecological lifestyles. *Molecular Ecology*, *28*(4), 721–730. doi: 10.1111/mec.14995

López-Mondéjar, R., Brabcová, V., Štursová, M., Davidová, A., Jansa, J., Cajthaml, T., & Baldrian, P. (2018). Decomposer food web in a deciduous forest shows high share of generalist microorganisms and importance of microbial biomass recycling. *ISME Journal*, *12*(7). doi: 10.1038/s41396-018-0084-2

López-Mondéjar, R., Zühlke, D., Větrovský, T., Becher, D., Riedel, K., & Baldrian, P. (2016). Decoding the complete arsenal for cellulose and hemicellulose deconstruction in the highly efficient cellulose decomposer Paenibacillus O199. *Biotechnology for Biofuels*, *9*(1), 104. doi: 10.1186/s13068-016-0518-x

Maillard, F., Andrews, Schreiner, K.M., E., Schilling, J., & Kennedy, P. (2020). Functional convergence in the decomposition of fungal necromass in soil and wood. *FEMS Microbiology*, *96*(2), doi: 10.1093/femsec/fiz209

McLaren, J. R., & Turkington, R. (2010). Ecosystem properties determined by plant functional group identity. *Journal of Ecology*, 98(2), 459–469. doi: 10.1111/j.1365-2745.2009.01630.x

Melillo, J. M., Aber, J. D., & Muratore, J. F. (1982). Nitrogen and lignin control of hardwood leaf litter decomposition dynamics. *Ecology*, *63*(3), 621–626. doi: 10.2307/1936780

Midgley, M. G., Brzostek, E., & Phillips, R. P. (2015). Decay rates of leaf litters from arbuscular mycorrhizal trees are more sensitive to soil effects than litters from ectomycorrhizal trees. *Journal of Ecology*, *103*(6), 1454–1463. doi: 10.1111/1365-2745.12467

Midgley, M. G., & Phillips, R. P. (2016). Resource stoichiometry and the biogeochemical consequences of nitrogen deposition in a mixed deciduous forest. *Ecology*, *97*(12), 3369–3377. doi: 10.1002/ecy.1595

748 Miltner, A., Bombach, P., Schmidt-Brücken, B., & Kästner, M. (2012). SOM genesis: Microbial
749 biomass as a significant source. *Biogeochemistry*, *111*(1–3), 41–55. doi: 10.1007/s10533-
750 011-9658-z

751 Mushinski, R. M., Phillips, R. P., Payne, Z. C., Abney, R. B., Jo, I., Fei, S., … Raff, J. D. (2019).
752 Microbial mechanisms and ecosystem flux estimation for aerobic NO y emissions from
753 deciduous forest soils. *Proceedings of the National Academy of Sciences of the United*
754 *States of America*, *116*(6), 2138–2145. doi: 10.1073/pnas.1814632116

755 Nguyen, N. H., Song, Z., Bates, S. T., Branco, S., Tedersoo, L., Menke, J., … Kennedy, P. G.
756 (2016). FUNGuild: An open annotation tool for parsing fungal community datasets by
757 ecological guild. *Fungal Ecology*, *20*, 241–248. doi: 10.1016/j.funeco.2015.06.006

758 Oksanen, J., Blanchet, F. G., Kindt, R., Legendre, P., Minchin, P. R., O'Hara, R. B., … Wagner,
759 H. (2013). vegan: Community Ecology Package. R package version 2.0-10. *R Package Ver.*
760 *2.4–3*.

761 Palmer, J. M., Jusino, M. A., Banik, M. T., & Lindner, D. L. (2018). Non-biological synthetic
762 spike-in controls and the AMPtk software pipeline improve mycobiome data. *PeerJ*, *6*,
763 e4925. doi: 10.7717/peerj.4925

764 Pankratov, T. A., Ivanova, A. O., Dedysh, S. N., & Liesack, W. (2011). Bacterial populations
765 and environmental factors controlling cellulose degradation in an acidic Sphagnum peat.
766 *Environmental Microbiology*, *13*(7), 1800–1814. doi: 10.1111/j.1462-2920.2011.02491.x

767 Phillips, R. P., Brzostek, E., & Midgley, M. G. (2013). The mycorrhizal-associated nutrient
768 economy: A new framework for predicting carbon-nutrient couplings in temperate forests.
769 *New Phytologist*, pp. 41–51. doi: 10.1111/nph.12221

770 Portillo-Estrada, M., Pihlatie, M., Korhonen, J. F. J., Levula, J., Frumau, A. K. F., Ibrom, A., …
771 Niinemets, Ü. (2016). Climatic controls on leaf litter decomposition across European forests
772 and grasslands revealed by reciprocal litter transplantation experiments. *Biogeosciences*,
773 *13*(5), 1621–1633. doi: 10.5194/bg-13-1621-2016

774 Prescott, C. E. (2010). Litter decomposition: What controls it and how can we alter it to
775 sequester more carbon in forest soils? *Biogeochemistry*, *101*(1–3), 133–149. doi:
776 10.1007/s10533-010-9439-0

777 Read, D. J., & Perez-Moreno, J. (2003). Mycorrhizas and nutrient cycling in ecosystems - A
778 journey towards relevance? *New Phytologist*, *157*(3), 475-492. doi: 10.1046/j.1469-
779 8137.2003.00704.x

780 Rognes, T., Flouri, T., Nichols, B., Quince, C., & Mahé, F. (2016). VSEARCH: A versatile open
781 source tool for metagenomics. *PeerJ*, *4*, e2584. doi: 10.7717/peerj.2584

Rosling, A., Midgley, M. G., Cheeke, T., Urbina, H., Fransson, P., & Phillips, R. P. (2016). Phosphorus cycling in deciduous forest soil differs between stands dominated by ecto- and arbuscular mycorrhizal trees. *New Phytologist*, *209*(3), 1184–1195. doi: 10.1111/nph.13720

Ryan M.E., Schreiner, K.M., Swenson, J.T., Gagne, J., & Kennedy, P.G. Chemical analysis shows dynamic changes during the degradation of ectomycorrhizal fungal necromass. Fungal Ecology, in revision.

Sangkhobol, V., & Skerman, V. B. D. (1981). Chitinophaga, a new genus of chitinolytic myxobacteria. *International Journal of Systematic Bacteriology*, *31*(3), 285–293. doi: 10.1099/00207713-31-3-285

Schäfer, H., Dannoura, M., Ataka, M., & Osawa, A. (2019). Decomposition rate of extraradical hyphae of arbuscular mycorrhizal fungi decreases rapidly over time and varies by hyphal diameter and season. *Soil Biology and Biochemistry*, *136*, 107533. doi: 10.1016/j.soilbio.2019.107533

Schweigert, M., Herrmann, S., Miltner, A., Fester, T., & Kästner, M. (2015). Fate of ectomycorrhizal fungal biomass in a soil bioreactor system and its contribution to soil organic matter formation. *Soil Biology and Biochemistry*, *88*, 120–127. doi: 10.1016/j.soilbio.2015.05.012

Shade, A., & Handelsman, J. (2012). Beyond the Venn diagram: The hunt for a core microbiome. *Environmental Microbiology*, *14*(1), 4–12. doi: 10.1111/j.1462-2920.2011.02585.x

Smith, G. R., & Wan, J. (2019). Resource-ratio theory predicts mycorrhizal control of litter decomposition. *New Phytologist*, doi.org/10.1111/nph.15884. doi: 10.1111/nph.15884

Sokal, R. . and R. (1970). Biometry. The principles and practice of statistics in biological research. In *Systematic Zoology*. doi: 10.2307/2412280

Solly, E. F., Schöning, I., Boch, S., Kandeler, E., Marhan, S., Michalzik, B., … Schrumpf, M. (2014). Factors controlling decomposition rates of fine root litter in temperate forests and grasslands. *Plant and Soil*, 382(1–2), 203–218. doi: 10.1007/s11104-014-2151-4

Soudzilovskaia, N. A., van der Heijden, M. G. A., Cornelissen, J. H. C., Makarov, M. I., Onipchenko, V. G., Maslov, M. N., … van Bodegom, P. M. (2015). Quantitative assessment of the differential impacts of arbuscular and ectomycorrhiza on soil carbon cycling. *New Phytologist*, *208*(1), 280–293. doi: 10.1111/nph.13447

Sterkenburg, E., Bahr, A., Brandström Durling, M., Clemmensen, K. E., & Lindahl, B. D. (2015). Changes in fungal communities along a boreal forest soil fertility gradient. *New Phytologist*, *207*(4), 1145–1158. doi: 10.1111/nph.13426

816 Strickland, M. S., Osburn, E., Lauber, C., Fierer, N., & Bradford, M. A. (2009). Litter quality is
817 in the eye of the beholder: Initial decomposition rates as a function of inoculum
818 characteristics. Functional Ecology, 23(3), 627–636. doi: 10.1111/j.1365-
819 2435.2008.01515.x

820 Taylor, D. L., Walters, W. A., Lennon, N. J., Bochicchio, J., Krohn, A., Caporaso, J. G., &
821 Pennanen, T. (2016). Accurate estimation of fungal diversity and abundance through
822 improved lineage-specific primers optimized for Illumina amplicon sequencing. *Applied*
823 *and Environmental Microbiology*, *82*(24), 7217–7226. doi: 10.1128/AEM.02576-16

824 Tláskal, V., Voříšková, J., & Baldrian, P. (2016). Bacterial succession on decomposing leaf litter
825 exhibits a specific occurrence pattern of cellulolytic taxa and potential decomposers of
826 fungal mycelia. *FEMS Microbiology Ecology*, *92*, 11. doi: 10.1093/femsec/iw177

827 Trivedi, P., Delgado-Baquerizo, M., Jeffries, T. C., Trivedi, C., Anderson, I. C., Lai, K., …
828 Singh, B. K. (2017). Soil aggregation and associated microbial communities modify the
829 impact of agricultural management on carbon content. *Environmental Microbiology*, *19*(8),
830 3070–3086. doi: 10.1111/1462-2920.13779

831 Vivanco, L., & Austin, A. T. (2008). Tree species identity alters forest litter decomposition
832 through long-term plant and soil interactions in Patagonia, Argentina. *Journal of Ecology*,
833 96(4), 727–736. doi: 10.1111/j.1365-2745.2008.01393.x

834 Warton, D. I., & Hui, F. K. C. (2011). The arcsine is asinine: The analysis of proportions in
835 ecology. *Ecology*, *92*(1), 3–10. doi: 10.1890/10-0340.1

836 Yilmaz, N., Lopez-Quintero, C. A., Vasco-Palacios, A. M., Frisvad, J. C., Theelen, B.,
837 Boekhout, T., Houbraken, J. (2016). Four novel Talaromyces species isolated from leaf
838 litter from Colombian Amazon rain forests. *Mycological Progress*, *15*, 1041–1056. doi:
839 10.1007/s11557-016-1227-3

840 Zeglin, L. H., Kluber, L. A., & Myrold, D. D. (2013). The importance of amino sugar turnover to
841 C and N cycling in organic horizons of old-growth Douglas-fir forest soils colonized by
842 ectomycorrhizal mats. *Biogeochemistry*, *112*(1–3), 679–693. doi: 10.1007/s10533-012-
843 9746-8

844 Zeglin, L. H., & Myrold, D. D. (2013). Fate of decomposed fungal cell wall material in organic
845 horizons of old-growth douglas-fir forest soils. *Soil Science Society of America Journal*,
846 *77*(2), 489–500. doi: 10.2136/sssaj2012.0204

847 Zhang, D., Hui, D., Luo, Y., & Zhou, G. (2008). Rates of litter decomposition in terrestrial
848 ecosystems: global patterns and controlling factors. *Journal of Plant Ecology*, *1*(2), 85–93.
849 doi: 10.1093/jpe/rtn002

Zhang, Z., Phillips, R. P., Zhao, W., Yuan, Y., Liu, Q., & Yin, H. (2019). Mycelia-derived C contributes more to nitrogen cycling than root-derived C in ectomycorrhizal alpine forests. *Functional Ecology*. doi: 10.1111/1365-2435.13236

Tables

Table 1. Site Characteristics. Climate Decomposition Index (CDI) is a multiplicative function developed by Adair *et al*., (2008) that describes the effect of monthly variation in temperature and water on decomposition, values range from 0 to 1, with higher values being indicative of faster rates of decay. See Supplementary Note 2 for more details on site CDI calculations.

Site	Latitude (°N)	Longitude (°W)	Climate Decomposition Index	Soil Description	Dominant Plant Species	Mycorrhizal Type	pH
Oak Savannah	45.425770	093.208520	0.2698	Outwash derived entisols with a fine sand texture	*Poa sp.*, *Ambrosia sp*., and *Agropyron sp.*	AM	5.3 ± 0.03
					Quercus ellipsoidalis and *Quercus macrocarpa*	EM	4.3 ± 0.04
Temperate Forest	39.083333	086.466667	0.3482	Sandstone derived inceptisols with a silty loam texture	*Acer saccharum*, *Liriodendron tulipifera*,*Prunus serotina* and *Sassafras albidu*	AM	4.7 ± 0.1
					Quercus rubra, Quercus velutina, Quercus alba Carya glabra and *Fagus grandifolia*	EM	3.4 ± 0.02

867 **Table 2.** Analyses of initial fungal necromass quality. Three independent replicates were analyzed
868 where standard errors are reported, otherwise values are based on a single replicate.

	High Quality *Mortierella elongata*	**Low Quality** *Meliniomyces bicolor*
	Elemental Analysis	
C (%)	49.4 ± 2.2	51.4 ± 0.3
N (%)	7.0 ± 1.5	3.8 ± 0.03
C/N	7.5 ± 1.6	13.7 ± 0.2
	GC/MS Analysis (%)	
Aromatic	6.2 ± 0.3	17.6
Lipid	44.7 ± 3.1	57.8
N-containing	10.3 ± 2.5	1.1
Sterol	0.0 ± 0.0	0.3
Sugar	29.3 ± 1.8	22.0
Unspecified	9.5 ± 0.3	1.3
	Melanin Analysis (%)	
Melanin	4.3	17.5

869
870
871
872
873
874
875
876
877

878 **Table 3**. Results from permutational multivariate analysis of variance (PERMANOVA) statistical
879 tests showing the effects of incubation time, vegetation type, necromass quality and their
880 interactions on Bray-Curtis and Euclidean dissimilarity matrices for both fungal and bacterial
881 communities at the oak savannah and temperate forest sites (*P≤0.05; **P≤0.01; ***P≤0.001).

Oak Savannah					**Temperate Forest**				
Fungi	*DF*	*F*	*R2*	*P*	*Fungi*	DF	F	R2	P
Incubation time	2	1.0855	0.02278	0.296	Incubation time	2	1.4466	0.03384	0.062
Vegetation type	1	14.1972	0.29800	0.001 ***	Vegetation type	1	6.1621	0.07207	0.001 ***
Necromass quality	1	1.6946	0.03557	0.086	Necromass quality	1	5.4378	0.06360	0.001 ***
Vegetation type x Incubation time	2	0.8849	0.01857	0.471	Vegetation type x Incubation time	2	1.2012	0.02810	0.178
Necromass quality x Incubation time	2	0.5539	0.01163	0.851	Necromass quality x Incubation time	2	1.1063	0.02588	0.293
Necromass quality x Vegetation type	1	1.5594	0.03273	0.136	Necromass quality x Vegetation type	1	2.1526	0.02518	0.014 *
Necromass quality x Vegetation type x Incubation time	2	0.6666	0.01399	0.737	Necromass quality x Vegetation type x Incubation time	2	0.6224	0.01456	0.964
Bacteria	*DF*	*F*	*R2*	*P*	*Bacteria*	*DF*	*F*	*R2*	*P*
Incubation time	2	2.9100	0.05658	0.005 **	Incubation time	2	4.4864	0.07647	0.001 ***
Vegetation type	1	4.0124	0.07802	0.002 **	Vegetation type	1	10.0354	0.08553	0.001 ***
Necromass quality	1	10.4038	0.20230	0.001 ***	Necromass quality	1	15.3718	0.13101	0.001 ***
Vegetation type x Incubation time	2	1.3648	0.02654	0.159	Vegetation type x Incubation time	2	1.3491	0.02300	0.110
Necromass quality x Incubation time	2	1.1701	0.02275	0.265	Necromass quality x Incubation time	2	1.9833	0.03381	0.011 *
Necromass quality x Vegetation type	1	1.6475	0.03204	0.092	Necromass quality x Vegetation type	1	4.6002	0.03921	0.001 ***
Necromass quality x Vegetation type x Incubation time	2	0.9183	0.01786	0.479	Necromass quality x Vegetation type x Incubation time	2	0.8444	0.01439	0.675

887 **Figure Legends**

888 **Figure 1.** Proportional mass remaining (mean ± 1 SE) for high-quality *Mortierella elongata* (light
889 shading) and low-quality *Meliniomyces bicolor* (dark shading) fungal necromass in AM-associated
890 vegetation (grey circles) and EM-associated vegetation (tan triangles) at the oak savannah (a) and
891 temperate forest (b) sites. At the oak savannah site, mass remaining was measured at four time
892 periods, 14, 28, 42 and 56 days (n=3 litter bags of each fungal species for each mycorrhizal
893 association treatment for each sampling date). At the temperate forest site, mass remaining was
894 measured at three time periods, 14, 31 and 92 days (n = 7 litter bags of each fungal species for
895 each mycorrhizal association treatment for each sampling date). Inset graphs show double
896 exponential decay curves for high- and low-quality necromass, as decomposition did not differ
897 between vegetation-mycorrhizal types. For measures of error around model parameter estimates
898 see Fig.S1.

899

900 **Figure 2.** Diversity indices (H) for bacterial and fungal communities in different habitats (in the
901 surrounding soil or on fungal necromass) at the oak savannah (a) and temperate forest (b) sites. H
902 values are also presented for bacterial and fungal communities under AM- and EM-associated
903 vegetation for soil and necromass habitats in the oak savannah (c & e) and temperate forest (d &
904 f). Differences in H values between microbial communities on high and low quality necromass
905 and for the different fungal necromass periods are shown for the oak savannah (g & i) and
906 temperate forest sites (h & j). The high-quality necromass species was *Mortierella elongata* and
907 the low-quality necromass species was *Meliniomyces bicolor*. ns refers to non-significant results;
908 *P≤0.05; **P≤0.01; ***P≤0.001; boxes that do not share similar letters denote statistical
909 significance, P<0.05.

Figure 3. Non-metric multidimensional scaling (NMDS) analysis of bacterial (a & b) and fungal (c & d) communities colonizing high- and low-quality necromass, as well as, in the soil under AM and EM-associated vegetation at the oak savannah (a & c) and temperate forest (b & d) sites. Small circles represent individual samples and large circles represent the centroids.

Figure 4. Relative abundances of necromass-associated bacterial (a) and fungal (b) guilds for the different vegetation types (AM- and EM-dominated vegetation), necromass qualities (high and low) and fungal necromass incubation periods (14, 28 and 42 days) in the oak savannah and temperate forest sites.

Figure 5. Fungal genera significantly impacted by the necromass quality type (high and low) depending of vegetation type (AM- and EM-dominated vegetation) in the oak savannah and temperate forest sites. Circles are coloured based on guild assignment and circle size is proportional to the relative abundance. Green highlights indicate fungal genera responding in the same way to the necromass species (high and low) within each site. Purple highlights indicate fungal genera responding in the same way to the necromass quality type (high and low) within and between sites.

Figure 6. Bacterial genera significantly impacted by the necromass quality type (high and low) depending on vegetation type (AM- and EM-dominated vegetation) in the oak savannah and temperate forest sites. Circles are colored based on guild assignment and circle size is proportional to the relative abundance. Green highlights indicate bacterial genera responding in the same way to the necromass species (high and low) within each site. Purple highlights indicate bacterial

933 genera responding in the same way to the necromass species (high and low) within and between
934 sites.
935
936
937
938
939
940
941
942
943
944
945
946
947
948
949
950
951
952

Figure 1.

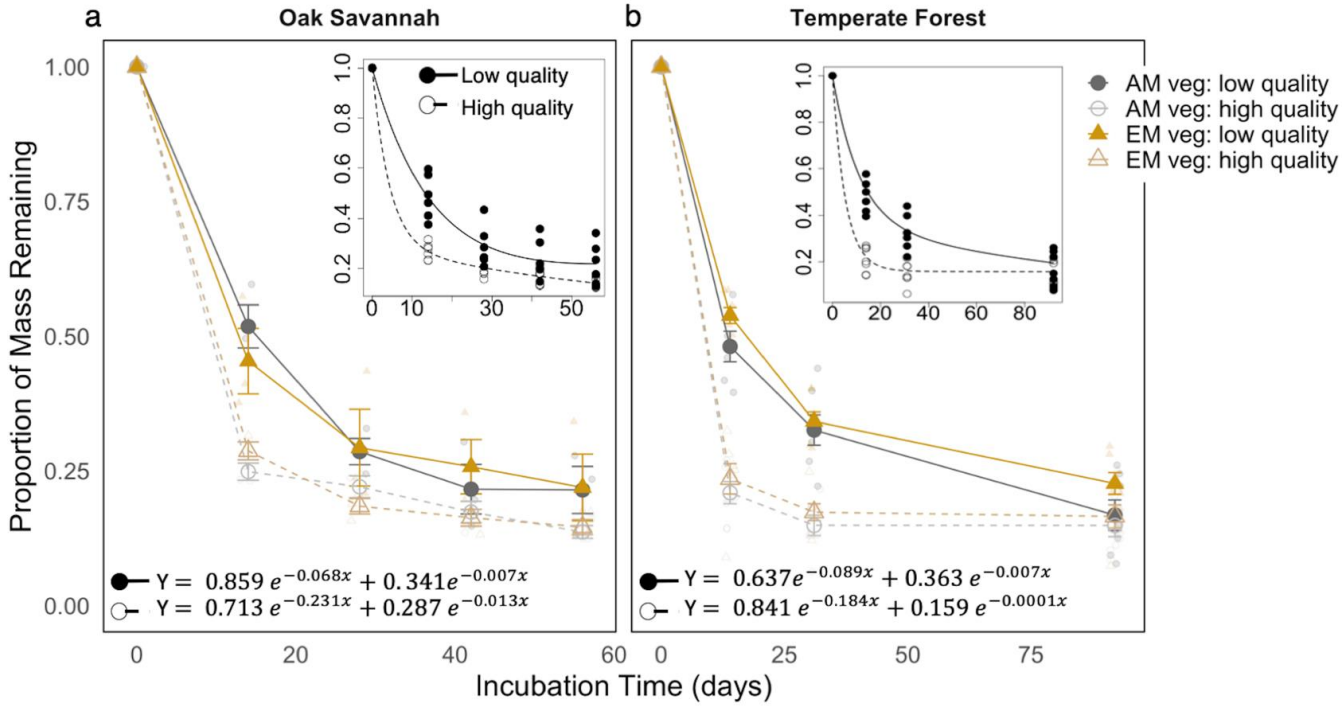
a
Oak Savannah
b
Temperate Forest
Low quality
High quality
AM veg: low quality
AM veg: high quality
EM veg: low quality
EM veg: high quality
Proportion of Mass Remaining
Incubation Time (days)
Y = 0.859 e^−0.068x + 0.341e^−0.007x
Y = 0.713 e^−0.231x + 0.287 e^−0.013x
Y = 0.637e^−0.089x + 0.363 e^−0.007x
Y = 0.841 e^−0.184x + 0.159 e^−0.0001x

Figure 2.

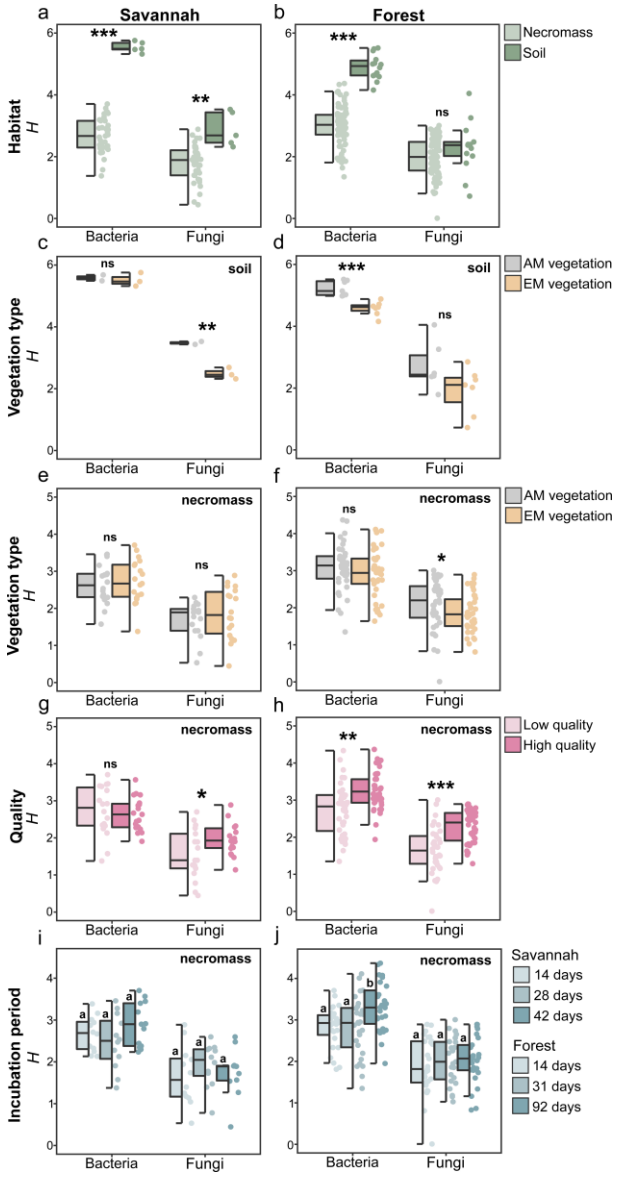
a
Savannah
b
Forest
Necromass
Soil
Habitat
H
***
**
ns
Bacteria
Fungi
c
d
soil
AM vegetation
EM vegetation
Vegetation type
e
f
necromass
g
h
Low quality
High quality
Quality
i
j
Incubation period
Savannah
14 days
28 days
42 days
Forest
14 days
31 days
92 days

Figure 3.

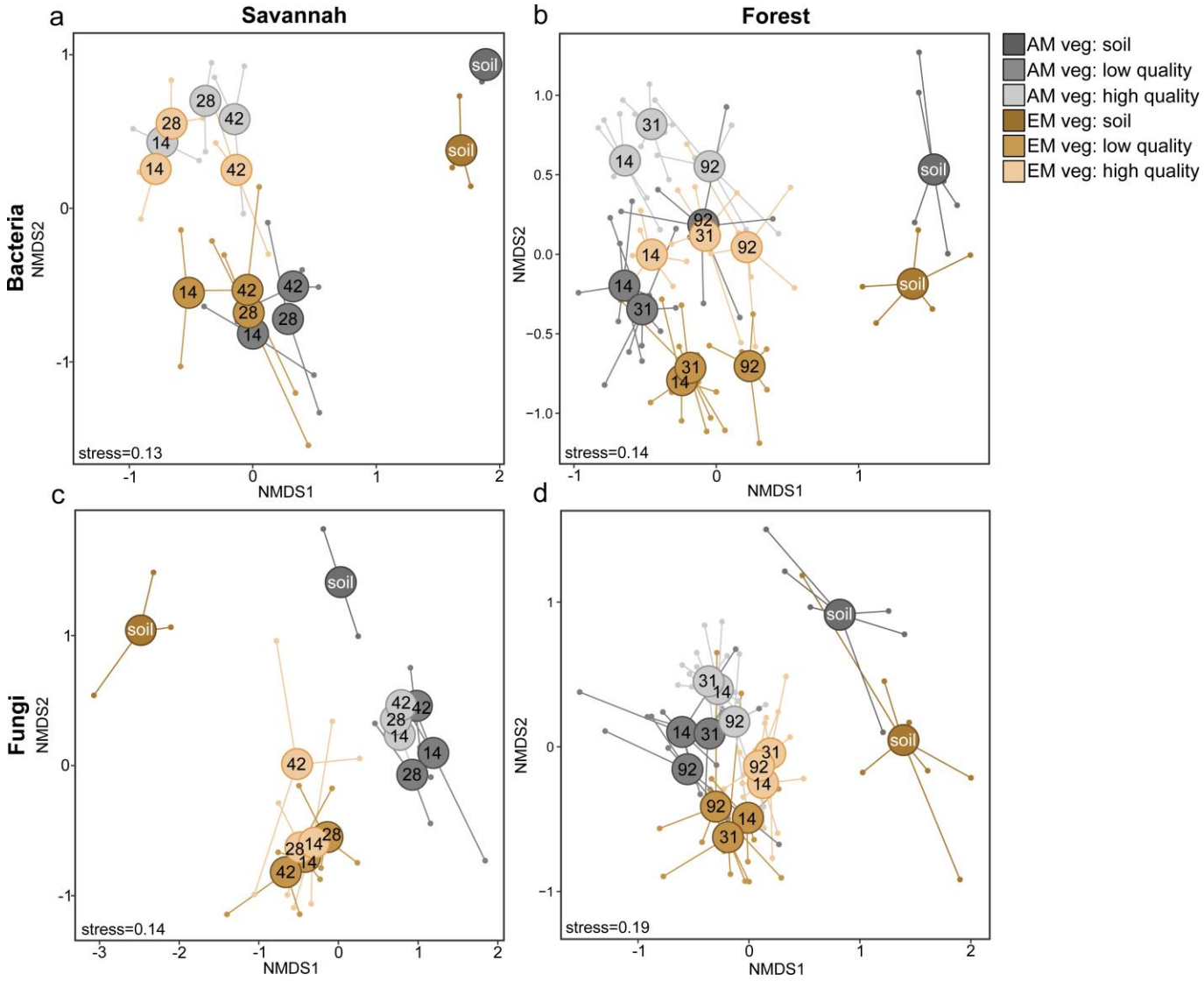
a
Savannah
b
Forest
c
d
Bacteria
Fungi
NMDS1
NMDS2
stress=0.13
stress=0.14
stress=0.14
stress=0.19
AM veg: soil
AM veg: low quality
AM veg: high quality
EM veg: soil
EM veg: low quality
EM veg: high quality

Figure 4.

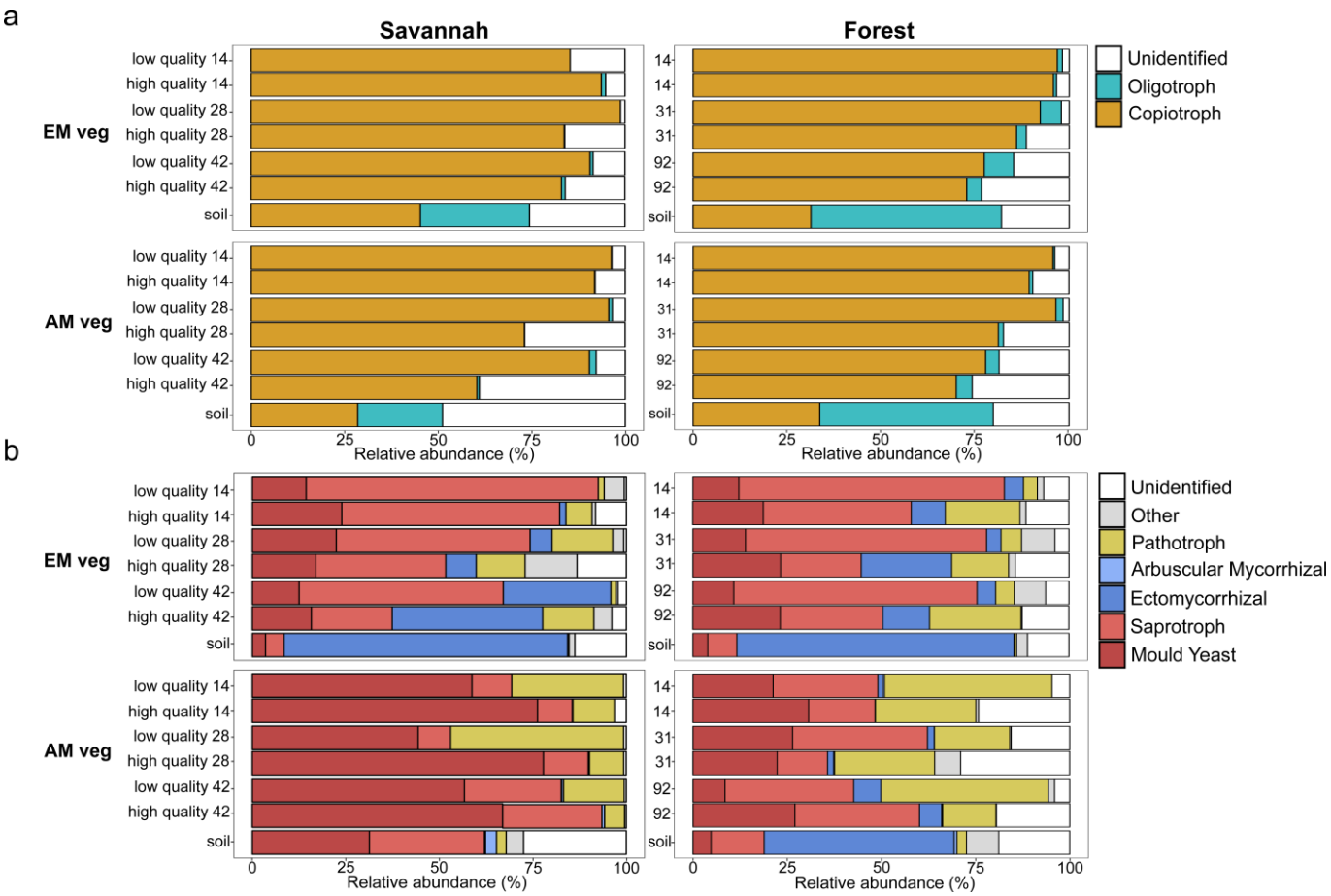
a
Savannah
Forest
EM veg
AM veg
low quality 14
high quality 14
low quality 28
high quality 28
low quality 42
high quality 42
soil
14
31
92
Unidentified
Oligotroph
Copiotroph
0
25
50
75
100
Relative abundance (%)
b
Unidentified
Other
Pathotroph
Arbuscular Mycorrhizal
Ectomycorrhizal
Saprotroph
Mould Yeast

Figure 5.

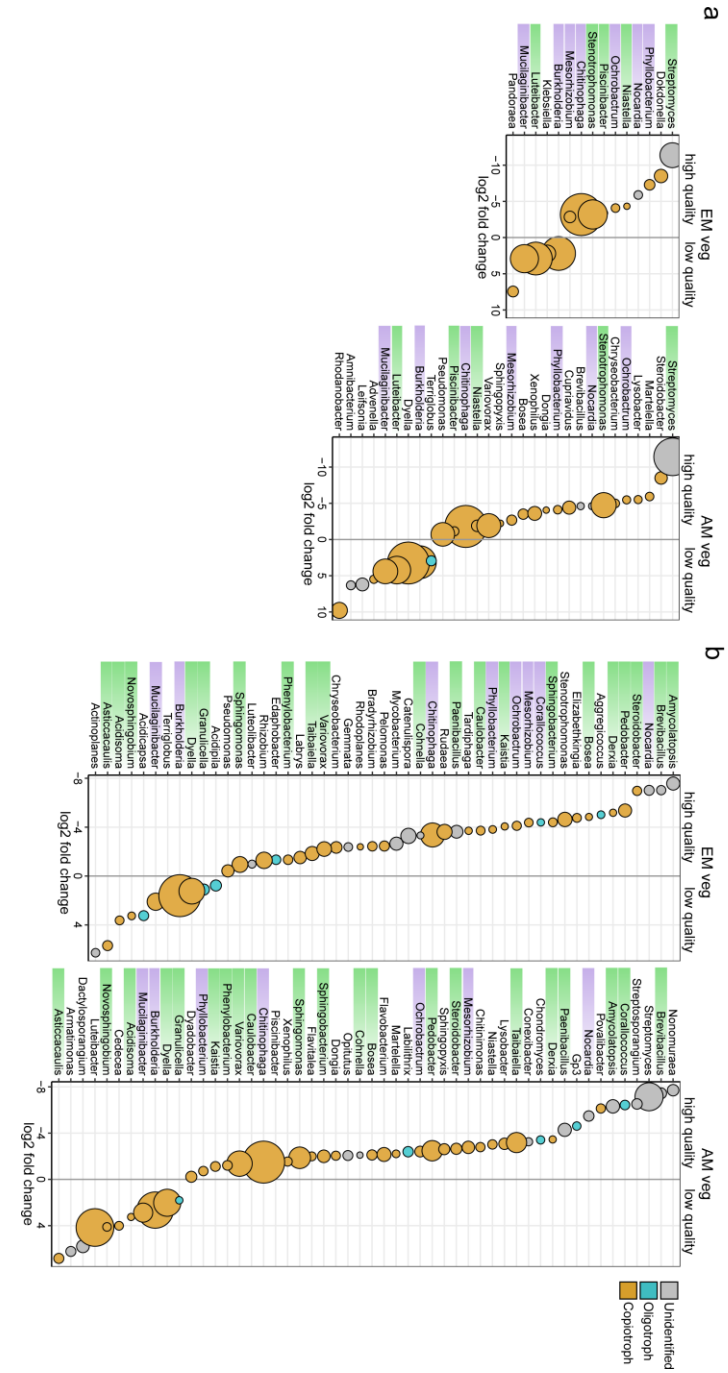
a
Savannah
Streptomyces
Dokdonella
Phyllobacterium
Nocardia
Nitrosomonas
Ochrobactrum
Pseudolabrys
Pseudonocardia
Stenotrophomonas
Chitinophaga
Mesorhizobium
Burkholderia
Klebsiella
Luteibacter
Mucilaginibacter
Pandoraea
high quality
EM veg
low quality
log2 fold change
−10
−5
0
5
10
Streptomyces
Steroidobacter
Martelella
Lysobacter
Ochrobactrum
Nitrosomonas
Chryseobacterium
Stenotrophomonas
Nocardia
Brevibacillus
Cupriavidus
Phyllobacterium
Dongia
Xenophilus
Bosea
Mesorhizobium
Sphingopyxis
Variovorax
Niastella
Chitinophaga
Pseudomonas
Pseudolabrys
Burkholderia
Dyella
Luteibacter
Mucilaginibacter
Aeromicrobium
Arenimonas
Ammibacterium
Rhodanobacter
high quality
AM veg
low quality
log2 fold change
−10
−5
0
5
10
b
Forest
Amycolatopsis
Brevibacillus
Nocardia
Steroidobacter
Pedobacter
Ochrobactrum
Aggregicoccus
Bosea
Elizabethkingia
Stenotrophomonas
Sphingobacterium
Coralococcus
Mesorhizobium
Ochrobactrum
Kaistia
Phyllobacterium
Caulobacter
Tardiphaga
Paenibacillus
Rubrobacter
Chitinophaga
Cohnella
Catenulispora
Mycobacterium
Pelomonas
Bradyrhizobium
Rhodoplanes
Solirubrobacter
Chryseobacterium
Variovorax
Taibaiella
Labrys
Phenylobacterium
Edaphobacter
Lutaibacter
Sphingomonas
Pseudomonas
Acidipila
Granulicella
Dyella
Burkholderia
Terriglobus
Mucilaginibacter
Acidicapsa
Acidisoma
Novosphingobium
Asticcacaulis
Actinoplanes
high quality
EM veg
low quality
log2 fold change
−8
−4
0
4
Nonomuraea
Brevibacillus
Streptomyces
Streptosporangium
Coralococcus
Amycolatopsis
Pedobacter
Nocardia
Gp3
Paenibacillus
Derxia
Chondromyces
Conexibacter
Lysobacter
Niastella
Chitinimonas
Mesorhizobium
Steroidobacter
Sphingopyxis
Rubrobacter
Ochrobactrum
Labilithrix
Martelella
Flavobacterium
Bosea
Cohnella
Gemmatimonas
Dongia
Sphingobacterium
Flavitalea
Sphingomonas
Xenophilus
Pseudolabrys
Edaphobacter
Chitinophaga
Caulobacter
Variovorax
Phenylobacterium
Kaistia
Phyllobacterium
Dyadobacter
Granulicella
Dyella
Burkholderia
Mucilaginibacter
Acidisoma
Cedecea
Novosphingobium
Lutaibacter
Dactylosporangium
Armatimonas
Asticcacaulis
high quality
AM veg
low quality
log2 fold change
−8
−4
0
4
Unidentified
Oligotroph
Copiotroph

1030 **Figure 6.**

1031